

Trends in the incidence of rain height and the effects on global satellite telecommunications

K. Paulson and A. Al-Mreri

University of Hull, Hull HU6 7RX, UK.

Abstract

Satellite communications using millimetre waves, in Ka band and above, experience significant fading by rain. Strong attenuation is experienced between the ground station and a level known as the rain height, in ITU-R recommendations assumed to be 360 m above the zero-degree isotherm (ZDI). This paper examines NOAA NCEP/NCAR Reanalysis 1 data to identify changes in the ZDI height over the last 30 years. Near the equator and the poles the ZDI height has been approximately stable over this period. However, in mid-latitudes, different regions show trends of increasing or decreasing ZDI height. Over the economically important regions of North America, China and Western Europe, the ZDI height has shown an increasing trend with peak rates in the range of 8 to 10 metres per year. Given a twenty-year life-time of a satellite system, this could lead to a 10 to 20% increase in fade intensity from a similar rain event. The effect will be compounded by increasing trends in the incidence of heavy rain recently identified in UK data. These trends will need to be considered when designing new systems.

Introduction

In temperate regions, most raindrops start as ice crystals that grow by sublimation at the expense of super-cooled water droplets via the Berganon Process, Yau and Rodgers [1].

23 As these particles grow, gravity exerts a stronger force and they fall through the
24 atmosphere, growing by collision and accretion. The particles begin to melt as they fall
25 into regions warmer than 0 degrees Celsius. In a stratified atmosphere this leads to a
26 layer, approximately one kilometre thick, containing mixed phase particles, known as the
27 melting layer, or as the bright band by radar meteorologists. Below the melting layer all
28 the ice has melted into raindrops. Depending on the height of the zero degree isotherm
29 (ZDI), an observer on the ground can experience ice, mixed phase or liquid hydrometeors.
30 An atmosphere experiencing strong convection may lead to a column of air with no
31 stratification containing mixed-phase particles throughout.

32 The atmosphere containing ice crystals above the melting layer has very low specific
33 attenuation at microwave and millimetre-wave frequencies. Below the melting layer, the
34 specific attenuation is due to scattering by raindrops and can be approximated as a power-
35 law of rain intensity e.g. Rec. ITU-R P.837-5 [2]. By contrast, the melting layer has
36 microwave specific attenuations many times that of the equivalent rain intensity due to
37 scattering by the large, water covered, melting particles; see Bråten et al [3].

38 Models of the average annual distribution of fade experienced by an Earth-space
39 microwave link needs to include attenuation by rain and the melting layer e.g. Rec. ITU-
40 R P.618-10 [4]. The fade due to rain depends upon the length of the Earth-space path
41 passing through the rain. This is generally assumed to be from the ground station to the
42 average annual rain height, h_R , provided by Rec. ITU-R P.839-3 [5]. The average annual
43 rain height is equated to the average annual ZDI height h_0 plus 360 m. Measurements of
44 the difference between ZDI and melting layer height have yielded values between 300 m,
45 Austin and Bemis [6]; and 900 m, Leary and Houze [7]. The difference depends upon
46 latitude, season and geography. The ITU-R provides two models for the average annual

47 distribution of actual rain height relative to the mean. These are both in table form and
48 are in Rec. ITU-R P.530-13 [8] for terrestrial links and Rec. ITU-R P.452-14 [9] for
49 Earth-space links. Both distributions are approximately Gaussian and assumed to apply
50 globally.

51 Over the last thirty years, it is very likely that the rain parameters that determine average
52 annual fade distributions have experienced significant change along with other well
53 recorded climate trends identified in reports of the UK Climate Impact Programme e.g.
54 UKCIP'09 Jenkins et al [10], and the Intergovernmental Panel on Climate Change [11].
55 A recent paper by Paulson [12] examining 20 years of high-resolution rain gauge data
56 from 30 sites in the southern UK, has identified significant increases in the incidence of
57 rain rates at the 0.01% and 0.001% exceedance levels. This has almost certainly led to a
58 doubling or tripling of outage rates on UK terrestrial links. It is also likely that increases
59 in ZDI height are increasing rain fade on Earth-space links. Increasing ZDI height leads
60 to increases the slant-path length affected by rain fading and hence larger rain fades.
61 Recently, Bradley et al [13] have noted 30-year increasing trends in ZDI height in the
62 tropics with gradients up to 6 m/year. General global warming is associated with ZDI
63 height increases. Diaz and Graham [14] noted a strong correlation between ZDI height
64 and tropical sea-surface temperature, while Harris et al [15] states that positive ZDI
65 height anomalies are linked to increasing planetary temperatures.

66 In this paper we examine global changes in the ZDI height over the last 30 years.
67 NCEP/NCAR Reanalysis data, produced by National Oceanic and Atmospheric
68 Administration (NOAA) is used. Section 2 introduces these data and provides some
69 evidence of its reliability. Section 3 examines global ZDI height trends. Section 4
70 considers the effects of these trends on Earth-space links.

71 **2 NOAA NCEP/NCAR Reanalysis 1**

72 The motivation for the NOAA NCEP/NCAR Reanalysis project was to address the
73 apparent climate change artefacts introduced by the occasional changes made to
74 numerical weather models, Kalnay et al [16]. Kalnay et al further state: “The basic idea
75 of the Reanalysis Project is to use a frozen state-of-the-art analysis/forecast system and
76 perform data assimilation using past data,”

77 The dataset provides a wide range of meteorological parameters over a global 2.5° grid at
78 6 hour intervals from 1948 to the present, calculated at 17 pressure levels. The global
79 grid has 73 latitudes and 144 longitudes. This project uses two reanalysis parameters: the
80 air temperature and altitude, both as a function of pressure level, averaged over each grid
81 square and sampled a 6-hour intervals. Diaz et al [17] conclude that the Reanalysis data
82 can reliably predict ZDI height, even over mountainous areas, over the period 1958 to the
83 present. Harris et al [15] found reasonable agreement between Reanalysis derived ZDI
84 height and bright band height measured using TRMM satellite data. Bradley et al [13]
85 identify tropical ZDI heights from Reanalysis data.

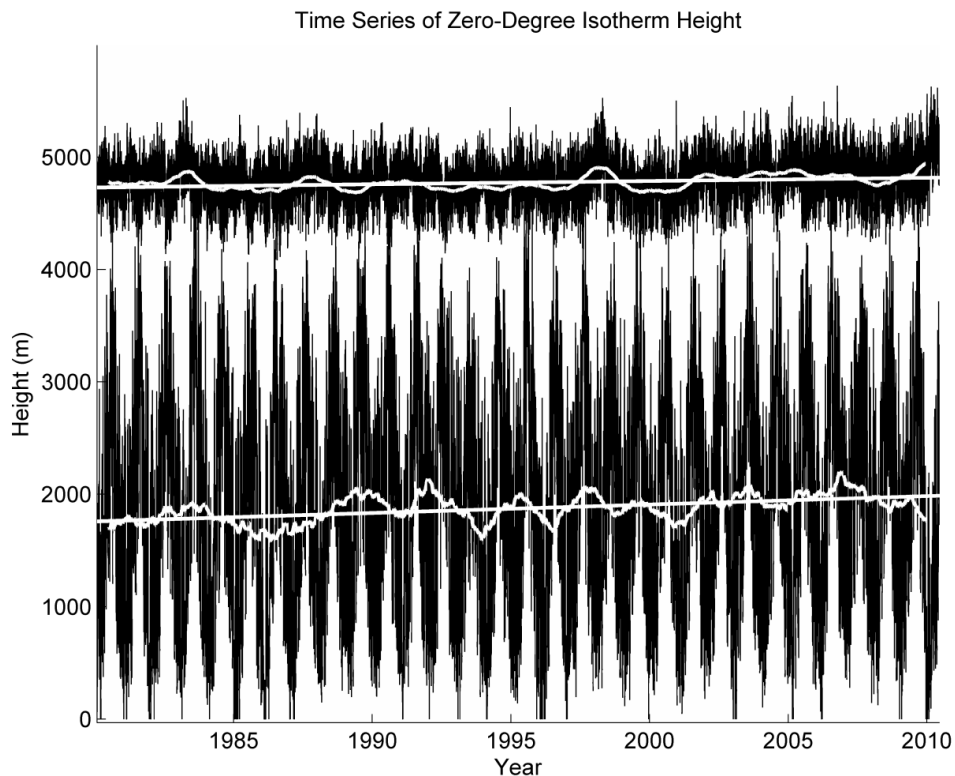
86 **3 Temporal Trends in Zero-Degree Isotherm Height**

87 The ZDI height has been calculated from the Reanalysis data by linear interpolation
88 between the lowest temperature-height points that decrease through zero Celsius with
89 increasing altitude. In high-latitude or high altitude regions the temperature at all
90 pressure levels can be below zero and in this case the ZDI height is taken as the ground
91 level and a flag is set.

92 A ZDI height has been calculated for each pixel for each 6-hour sample, from the
93 beginning of 1980 to mid-2010. Furthermore, running yearly means of ZDI height have

94 been calculated by temporal averaging the 1460 ZDI height samples centred on the 6-
95 hourly sample of interest. Figure 1 illustrates typical time-series of ZDI height for two
96 grid squares: both on the Greenwich meridian, one on the equator and the other on the
97 latitude of Edinburgh (55° North).

98



99

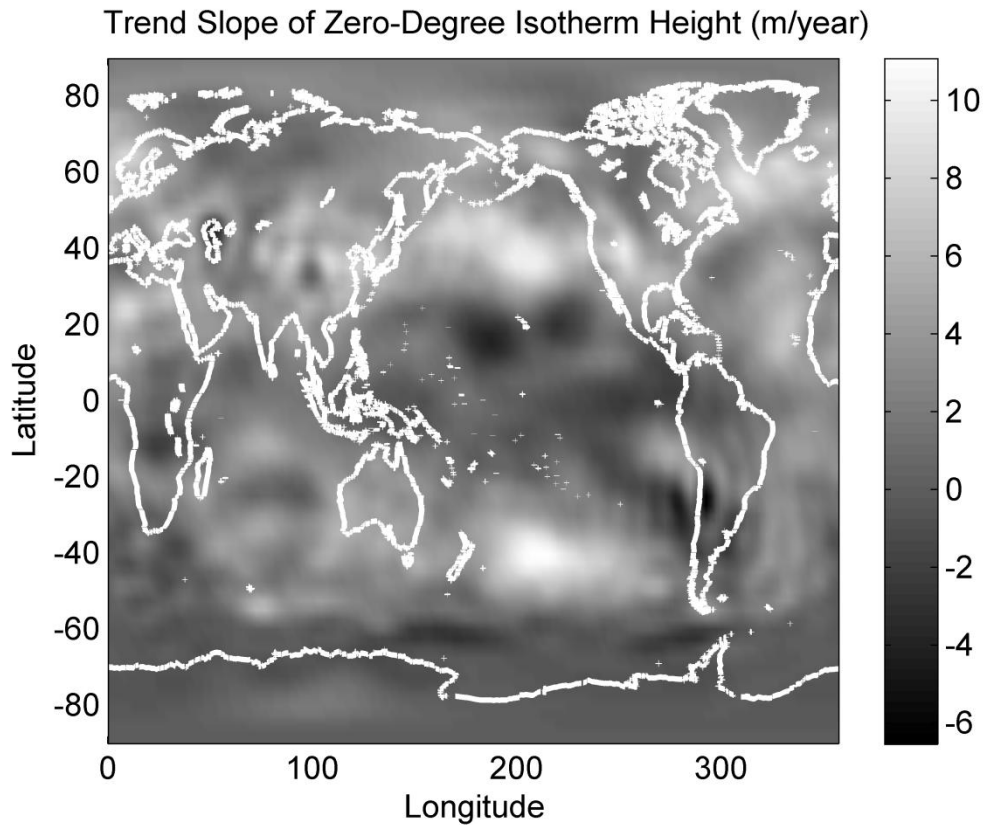
100 Figure 1: time-series of ZDI height for two grid squares centred on 0° of longitude and 0°
101 latitude (black, upper) and 55° (black, lower). The variable white lines represent the
102 running yearly average while the white straight lines are the least squares fit to the
103 running annual average.

104 Figure 1 illustrates general features of ZDI height. The ZDI is at its greatest average
105 height in warmer regions near the equator. Over each 12-month period the ZDI height
106 exhibits a near sinusoidal oscillation where it is below the mean during winter and above

107 the mean over summer. This oscillation has low amplitude near the equator where the
108 seasonal temperature variations are small, and the amplitude is larger at mid-latitudes. At
109 high latitudes the ZDI height is constrained by the Earth's surface and the oscillation
110 becomes asymmetric.

111 The 55° latitude ZDI height time-series shows a clear increasing trend consistently across
112 the 30-year period spanned by the data. The probability of the apparent trend being due
113 to random variation can be estimated using the Pearson correlation test and the non-
114 parametric Mann-Kendal trend test, see Önöz and Bayazit [18]. Both these tests yield a
115 probability of the observed trend being due to chance less than 10^{-8} . The least squares
116 (LSQ) linear regression line fitted to the running annual mean has a slope of 8 m/year
117 consistent in an increase in mean ZDI height of 240 m over the 30 year analysis period.
118 The yearly running average ZDI height increases from 1764 m in the calendar year 1980
119 to 1979 m in 2008. Rec. ITU-R P.839-3 provides an estimate of this parameter of 2095
120 m. The observed trend is an approximate 12% increase in average annual ZDI height,
121 from the 1980 value, that would have produced a similar increase in log rain fade on
122 Earth-space links.

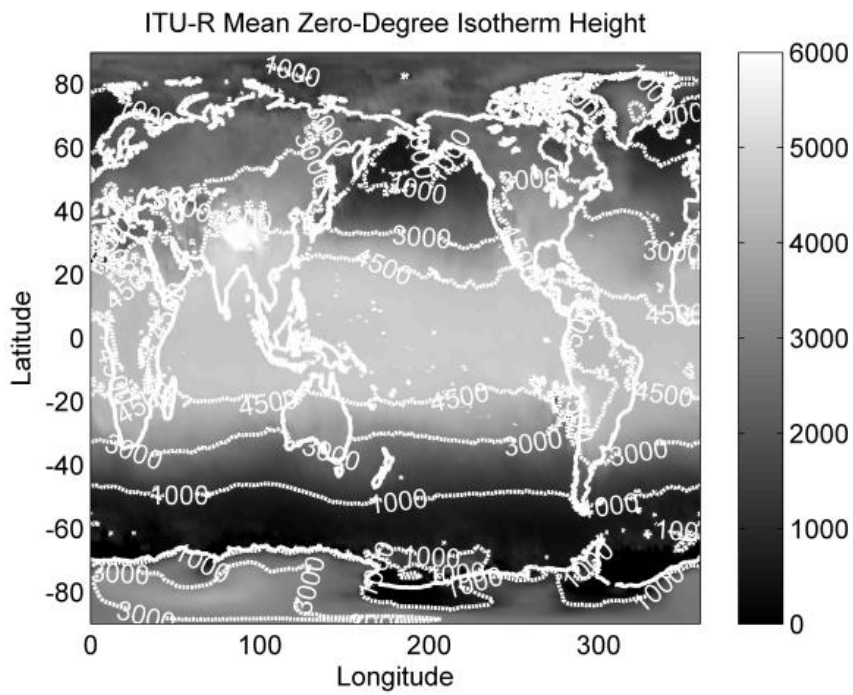
123 The same analysis was performed on all the grid squares in the dataset. Figure 2
124 illustrates the slope of the LSQ linear regression to the running annual mean ZDI height
125 for all the grid squares. Close to the equator the trend slopes are small and may be due to
126 random variation. At mid-latitudes i.e. around 40° north and south, strong increasing
127 trends are observed with a peak value of 10 m/year. A region of strongly increasing ZDI
128 height can be observed spanning the UK and Scandinavia. Extremes of both increasing
129 and decreasing trends occur over the Pacific Ocean. Harris et al [15] notes positive ZDI
130 height anomalies in the Pacific associated with El Niño.



131

132 Figure 2: slope of least squares linear regression to the running annual average ZDI
 133 height.

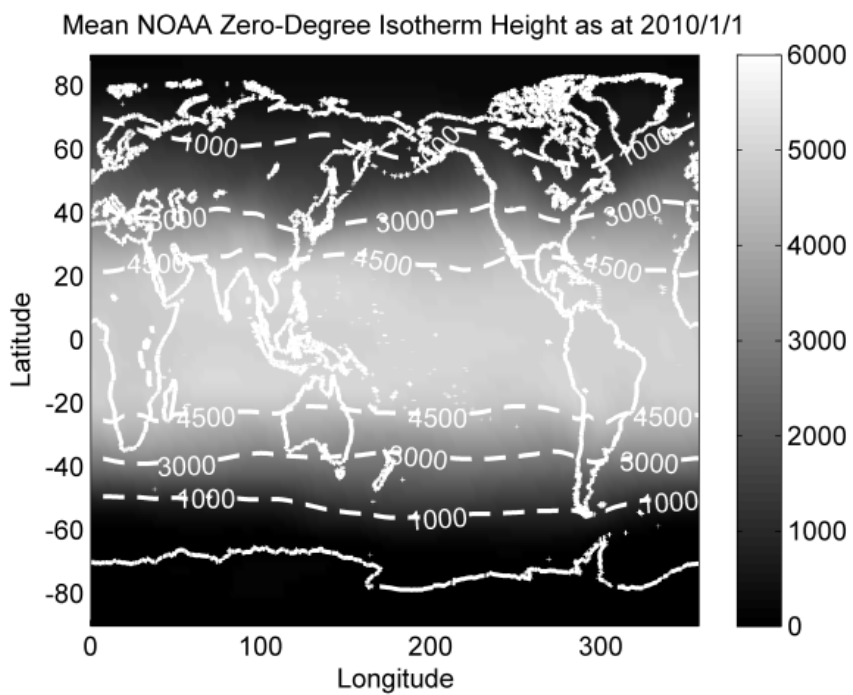
134 Figures 3 compare the average annual ZDI height in 2010 with the value provided by
 135 Rec. ITU-R P.839-3. The 2010 value was calculated by evaluating the LSQ linear
 136 regression at 1/1/2010. Bi-linear interpolation was used to estimate the values of the Rec.
 137 P.839 ZDI heights, averaged over 1.5° pixels, at the centres of the 2.5° NOAA grid-
 138 squares. The finer model grid used in Rec. P.839 data shows features around the
 139 Himalayas not present in the NOAA derived data. Large differences also occur near the
 140 poles, in central Asia and central North America. Over latitudes from 40° north to 40°
 141 south, the NOAA data are on average 300 m higher than Rec. P.839 values. These
 142 differences are due to modelling and assimilated data differences. The consistency
 143 imposed on the reanalysis data means that it is very likely that the observed trends are
 144 real, despite the altitude offset.



145

146

Fig. 3(a)



147

148

Fig. 3(b)

149 Figure 3: Zero-degree isotherm height as provided by (a) Rec. ITU-R P.839-3 and (b)
150 derived from NOAA Reanalysis data. The contour lines correspond to altitudes of 1000,
151 3000 and 4500 m and are increasing from the poles to the equator.

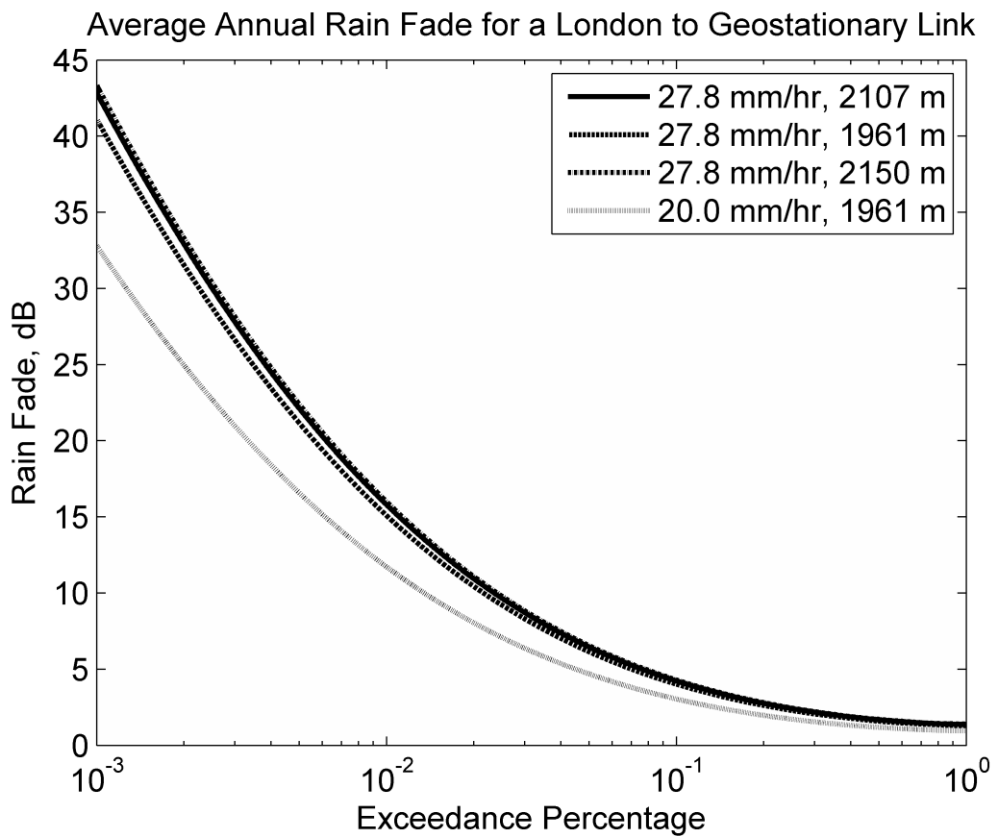
152 **4 Effects of Zero-Degree Isotherm Height Increase on Satellite Links**

153 The average annual rain fade distribution experienced by an Earth-space microwave link
154 can be estimated using ITU-R Rec. 618-10. The model has a large number of input
155 parameters including average annual rain height and the one-minute rain rate exceeded
156 for 0.01% of an average year. Figure 4 illustrates the predicted one-minute, rain fade
157 distributions for a notional circularly polarised Ka-band uplink operating at 27.5 GHz,
158 between a London ground station and a geostationary satellite at 0° longitude. The
159 calculation used a 0.01% exceeded rain rate of 27.8 mm/hr. This value comes from the
160 Bath Study, Howell and Watson [19] and is the figure used by the UK spectrum regulator
161 Ofcom for link coordination. Most of the Bath Study rain rate data was acquired over the
162 period 1986 to 2000. The annual average ZDI height provided by Rec. ITU-R P.839-3 is
163 2107 m.

164 Also illustrated are the distributions using the mean rain height calculated from the linear
165 regression to the London ZDI height, as at 1990 and 2010. During this 20 year period the
166 London annual mean ZDI height increased from 1961 m to 2150 m. The associated rain
167 fade level exceeded 0.01% of time has increased from 15.1 dB to 16.0 dB over this
168 period. At higher latitudes the greater proportionate increase in rain height will yield
169 greater proportionate increase in rain fade.

170 A recent paper by Paulson [12] shows the 0.01% rain rate averaged over the southern UK
171 has increased by 10 mm/hr from 19 to 29 mm/hr, over the period 1988 to 2008. Any
172 increases in 0.01% exceeded rain rate will exacerbate the trends illustrated in Fig 4. Also

173 plotted is the 1990 distribution using the 0.01% exceeded rain rate of 20 mm/hr. The
 174 increasing 0.01% exceeded rain rate and increasing rain height over this period leads to
 175 an increase in average annual rain fade, at the 0.01% exceedance level, of 4.3 dB from
 176 11.7 dB to 16.0 dB.



177
 178 Figure 4: Average annual rain fade distribution for a notional 27.5 GHz, circularly
 179 polarised uplink from London to a geostationary satellite at 0° longitude.

180 **6 Conclusions**

181 Current ITU-R models of rain height assume a time-invariant annual mean level. The
 182 rain rate exceeded 0.01% of the time is also assumed to be constant. Both these
 183 assumptions may be inadequate for the design of satellite communications systems.

184 Analysis of NOAA reanalysis data has provided strong evidence of multi-decade trends in
 185 ZDI height with increasing gradients as large as 10 m/year. In some regions decreasing

186 trends exist. Over economically important areas such as North America, northern Europe
187 and central Asia, these increasing trends would have increased rain height by 100 m to
188 200 m over the 20-year life-time and a satellite system, leading to a 10% to 20% increase
189 in rain fade.

190 Increasing trends in both 0.01% exceeded rain rate and rain height both lead to increasing
191 trends in 0.01% exceeded rain fade and need to be factored in when calculating link
192 budgets and cost-benefits of future satellite systems. The UK is experiencing increases in
193 ZDI height and in the incidence of heavy rain, both leading to increase in rain fade. The
194 increasing incidence of heavy rain is the dominant mechanism. In this extreme case,
195 average annual 0.01% exceeded rain fade could have doubled over the period 1990 to
196 2010. In practise, this trend would be obscured by large year-to-year and site-to-site
197 variation.

198 It is likely that the parameters used in many current ITU-R recommendations for the
199 design and coordination of telecommunications networks, are not stationary but are
200 exhibiting multi-decade trends. Even the definition of average annual parameters such as
201 rain height and rain rate distributions, needs to be reconsidered when stationarity is not
202 assumed. Different statistical techniques are required when deriving these parameters
203 from data spanning many years. Many ITU-R recommendations may need to be reframed
204 in terms of time-varying, expected distributions.

205 The effects of ZDI height increases are likely to be more dramatic on terrestrial fixed
206 links. In latitude and altitude combinations that spend parts of the winter with air
207 temperatures near the ground close to freezing, temperature increases and the associated
208 ZDI height increase could dramatically increase rain fade. Precipitation that was
209 previously frozen and associated with very low specific attenuations will instead be

210 composed of heterogeneous mixtures of ice and water, known as sleet in Europe, with
211 specific attenuations up to four times that of rain with the same accumulation rate.

212 **Acknowledgement**

213 NCEP Reanalysis data provided by the NOAA/OAR/ESRL PSD, Boulder, Colorado,
214 USA, from their Web site at <http://www.esrl.noaa.gov/psd/>

215 **References**

- 216 1. Yau, M. K., and Rodgers, R. R.; “A Short Course in Cloud Physics”, Butterworth-
217 Heinemann., 1989, ISBN 0-75-0632151.
- 218 2. Rec. ITU-R P.837-5, “Characteristics of precipitation for propagation modelling”, 2008.
- 219 3. L. Bråten, L., Tjelta T., and Larsen D., “Excess attenuation caused by sleet on costal
220 terrestrial radio links in Norway”, R&D N 66/2003, 2003, Telenor scientific document,
221 ISSN 0809-1021.
- 222 4. Rec. ITU-R P.618-10, “Propagation data and prediction methods required for the design
223 of Earth-space telecommunication systems”, 2010.
- 224 5. Rec. ITU-R P.839-3, “Rain height model for prediction methods”, 2002.
- 225 6. Austin, P. and Bemis, A., “A quantitative study of the “bright band” in radar
226 precipitation echoes”, J. Meteor., 1950, 7, pp 145–151.
- 227 7. Leary, C. A. and Houze, R. A., “Melting and evaporation of hydrometeors in precipitation
228 from the anvil clouds of deep tropical convection”, 1979, J. Atmos. Sci., 36, pp 669–679.
- 229 8. Rec. ITU-R P.530-13, “Propagation data and prediction methods required for the design
230 of terrestrial line-of-sight systems”, 2009.
- 231 9. Rec. ITU-R P.452-14, “Prediction procedure for the evaluation of interference between
232 stations on the surface of the Earth at frequencies above about 0.1 GHz”, 2010.

- 233 10. Jenkins, G. J., Perry, M.C., and Prior, M.J.O., “The climate of the United Kingdom and
234 recent trends”, Met Office Hadley Centre, 2007, Exeter, UK.
- 235 11. IPCC, <http://ipcc-wg1.ucar.edu/wg1/wg1-report.html>, 2007.
- 236 12. Paulson, K. S., “Trends in the incidence of rain rates associated with outages on fixed
237 links operating above 10 GHz in the southern United Kingdom”, *Radio Sci.*, 2010, 45,
238 RS1011, doi:10.1029/2009RS004193.
- 239 13. Bradley, R.S., Keimig, F. T., Diaz H. F. and Hardy, D. R., “Recent changes in freezing
240 level heights in the Tropics with implications for the deglaciation of high mountain
241 regions”, *Geophysical Research Letters*, 2009, 36, L17701, doi:10.1029/2009GL037712,
242 2009.
- 243 14. Diaz, H., and Graham, N., “Recent changes in tropical freezing heights and the role of sea
244 surface temperature”, *Nature*, 1996, 383, pp 152–155.
- 245 15. Harris JR., G. N., Bowman, K. P. and Dong-Bin Shin, “Comparison of Freezing-Level
246 Altitudes from the NCEP Reanalysis with TRMM Precipitation Radar Bright Band Data”,
247 *Journal of Climate*, 2000, 13:23, pp 4137-4148.
- 248 16. Kalnay E., Kanamitsu, M., Kistler, P. Collins, W. Deaven, D. Gandin, L. Iredell, M. Saha,
249 S. White, G. Woollen, J. Zhu, Y. Cheillab, M, Ebsuzaki, W. Higgins, W. Janowiak, J.
250 Mo, K. C. Ropelewski, C. Wang, J. Leetma, A. Reynolds, P. Jenne 1. and Joseph, D.
251 “The NCEP/NCAP 40-year reanalysis project”, *Bull. Amer. Meteor. Soc.*, 1996, 77, pp
252 437-470.
- 253 17. Diaz, H. F. Eischeid, J. K. Duncan C. and Bradley, R. S., “Variability of freezing levels,
254 melting season indicators, and snow cover for selected High-elevation and continental
255 regions in the last 50 years”, *Climatic Change*, 2003, 59, pp 33–52.
- 256 18. Önöz, B. and Bayazit, M., “The power of statistical test for trend detection”, *Turkish J.*
257 *Eng. Env. Sci.*, 2003, 27, pp 247-251.

258 19. Howell, R.G. and Watson, P.A., “Rainfall intensity data for use in prediction of
259 attenuation on terrestrial fixed links”, final report for the Radiocommunications Agency
260 under Research Contract AY 3362, 2001,
261 <http://www.ofcom.org.uk/static/archive/ra/topics/fixedlnk/members/rsspwg/docs2001/02->
262 [08-01/phase3finalreport.pdf](http://www.ofcom.org.uk/static/archive/ra/topics/fixedlnk/members/rsspwg/docs2001/02-08-01/phase3finalreport.pdf).